Atomic structure and line broadening of He-like ions in hot and dense plasmas

Michel Koenig, Philippe Malnoult, and Hoe Nguyen
Département de Recherches Physiques, Spectronomie des Gaz et des Plasmas, Université Pierre et Marie Curie, 4 place Jussieu, 75252 Paris Cédex 05, France
and Groupement de Recherches Coordonnées de l'Interaction Laser-Matière du CNRS, Ecole Polytechnique, 91120 Palaiseau, France
(Received 14 December 1987)

In this paper we present a self-consistent-field calculation for energy levels of He-like ions immersed in dense and hot plasmas. Exchange and correlation energies between bound electrons are shown to be much less perturbed than the single-particle energy. Concurrently, a fully quantum-mechanical impact calculation has been made to obtain the matrix elements of the complex electron line-broadening operator Γ_e. In the special case of the principal series, it is shown that the line shifts given by the two approaches are in good agreement for typical electron temperatures and densities of laser plasmas.

I. INTRODUCTION

The plasmas created by focusing high-power laser beams on planar or spherical targets are nonideal in the sense that the Coulomb interactions between particles exceed their thermal energy.[1] Therefore, the treatment of most of the physical problems in dense plasmas, such as electron transport, stopping power, equation of state, and line broadening, etc., is subordinated by the knowledge of elementary atomic processes.[2] The high-density and high-temperature conditions achieved in such plasmas ($N_e > 10^{23}$ cm^{-3}, $T_e > 100$ eV) involve, for example, a special study of electron bound states for charged radiators and their collisions with the surrounding particles.[3] The bound energy levels are shifted into the continuum by pressure ionization and the emission lines present a small red shift due to the local polarization of the plasma by the emitter (the so-called plasma polarization shift[4]). Recently such line shifts have been observed experimentally by using either a very low-Z planar target[5] or a neon-filled microballoon.[6] For a clear understanding of this optical effect and of several thermodynamic properties[2] in plasmas with coupling parameter $\Gamma \geq 1$, it is necessary to improve the theory describing the atomic systems immersed in finite-temperature and finite-density environments.[3,7,8]

Emission spectroscopy is a useful technique for the study of laser plasmas. It is especially used to diagnose electron density and temperature. To this end, many authors[9-11] have pointed out the necessity of simultaneously studying several line profiles. Among many possible choices, the K shell[12] is proved particularly interesting because its intense spectrum is relatively simple and easy to model. In fact, most of theoretical papers[3,13-14] concern H-like ions for which unperturbed atomic parameters are exactly known and attention can be focused on actual plasma effects. Comparatively very few works[15] have dealt in detail with He-like ions, the principal series of which is frequently more intense than the Lyman series in the same spectral interval. The present paper is intended to fill this gap. Specifically we will be interested in density and temperature effects caused by the free electrons surrounding a He-like emitter in plasmas created by lasers. In Sec. II we define the so-called confined atom using a self-consistent ion sphere model. Then we investigate the electron density and temperature effects on various atomic parameters, especially that on exchange and correlation energy which are specific to many bound electron systems. In order to take into account the line-broadening process, we shall consider in Sec. III the quantum-mechanical expression of the relaxation operator.[16] By using the Coulomb-Born-Oppenheimer approximation we show that the linewidth can be simply written as the difference between a "total width" free from plasma effects and a "correlation width" which contains effects due to long-range screening and the finite duration of the collision.[13] Finally, in Sec. IV, we show that the line shifts given by the imaginary part of the relaxation operator are in agreement with those obtained within the framework of the atomic model, provided that the electron density at the boundary surface $\rho_e(R_0)$ is used instead of N_e.

II. SELF-CONSISTENT-FIELD MODEL

In a previous paper[3] we noted that the typical times for the ion and electron component differ by about two orders of magnitude. Therefore it is possible to distinguish the different ways by which the electron bound states can be perturbed. The ion effects can be treated separately by means of either the quasistatic Stark effect[13,14] or the adiabatic approximation including ion dynamics.[17] On the other hand, the free electrons accomplish many oscillations during the effective lifetime of atomic states. Hence a self-consistent-field method provides a good framework for calculating their effects. In this paper, we shall use the so-called ion sphere model[3,8,18] which is based on the following principles: the atom is represented by a point-charge nucleus Z embedded in a spherical cavity containing enough electrons to ensure global neutrality. The ion

sphere radius R_0 is determined by the total ion density N_i [$R_0=(3/4\pi N_i)^{1/3}$]. Beyond this radius, the plasma is assumed to produce an electrically neutral background. Here we shall consider a fixed number of bound electrons N in order to treat in detail the spectrum of a given species. The problem now consists of solving self-consistently the wave equation and the Poisson equation relative to the bound electrons and free charged particles, respectively.

The solution of Poisson equation can be written in its integral form as

$$V(r)=-\frac{Z}{r}+\int_{r'<R_0}\frac{\rho(r')d\mathbf{r}'}{|\mathbf{r}-\mathbf{r}'|} . \tag{1}$$

On the right-hand side of Eq. (1), the first term denotes the contribution of the nucleus while the second arises from the total number density of electrons

$$\rho(r')=\rho_e(r')+\rho_b(r') . \tag{2}$$

Generally, Boltzmann statistics can be used because the temperatures T_e in the emission zone are much higher than the Fermi temperature $T_F=7.9$ eV $[10^{-23}N_e\ (\mathrm{cm}^{-3})]^{2/3}$. Therefore the number density of free electrons $\rho_e(r)$ is given by

$$\rho_e(r)=\rho_e(R_0)\frac{4}{\sqrt{\pi}}\int_{p_0}^{\infty}\frac{p^2}{(2mkT_e)^{3/2}}dp \times\exp\left[-\frac{1}{kT_e}\left[\frac{p^2}{2m}+V(r)+Q(r)\right]\right] , \tag{3}$$

where

$$p_0=p_0(r)=\{-2m[V(r)+Q(r)]\}^{1/2}$$

and the momentum condition $p\geq p_0$ ensures that the kinetic energy of free electrons is larger than the (negative) potential energy. In Eq. (3), $V(r)$ is the total electrostatic potential and $Q(r)$ is the quantum-mechanical correction[19–21] which takes into account the exchange correlation and density gradient effects. Integrating over p and introducing $x=(p_0^2/2mkT_e)^{1/2}$, we obtain from Eq. (3)

$$\rho_e(r)=\rho_e(R_0)B(x) , \tag{4}$$

where $B(x)$ is the Boltzmann factor defined by

$$B(x)=2x\pi^{-1/2}+\exp(x^2)\mathrm{erfc}(x) . \tag{5}$$

For a more accurate calculation based on Fermi-Dirac statistics, the standard Fermi function should be used instead of $B(x)$. In fact, we have verified that this numerical improvement is of no significance for the plasma parameters we consider here ($T_e\geq 100$ eV, $N_e\leq 10^{24}$ cm^{-3}).

The boundary conditions $V(r)=0$ and $Q(r)=0$ for $r\geq R_0$ imply that $B(x_{R_0})=1$. Consequently the electron density defined at the edge of the ion sphere can be written as

$$\rho_e(R_0)=N_e\exp(\beta\mu)/\exp(\beta\mu_0) , \tag{6}$$

where μ_0 (μ) denotes the chemical potential for the uniform (nonuniform) electron gas, respectively. The electrical neutrality condition

$$Z-N=4\pi\int_0^{R_0}r^2\rho_e(r)dr \tag{7}$$

associated with the inequality $B(x)\geq 1$ for $r\leq R_0$, shows that the boundary density $\rho_e(R_0)$ is always lower than the mean electron density N_e.

Then, in order to define our model completely, we have to consider the wave equation for the bound electrons. Owing to the spherical symmetry of the average potential due to the surrounding particles, the Hartree-Fock method is very suitable for a detailed description of the atomic system. So the bound electron eigenvalues and wave functions are obtained by solving the following system of coupled radial equations for each subshell i:

$$\left[\frac{d^2}{dr^2}-U_i(r)-\frac{l_i(l_i+1)}{r^2}-\varepsilon_i\right]P_i(r)=W_i(r) . \tag{8}$$

Here $U_i(r)$ is the potential function which takes into account the contribution of the nuclear charge, the perturbation due to the free electron gas, the direct part of the electrostatic interaction, and the exchange between equivalent electrons. $W_i(r)$ denotes a nonlocal function which includes the exchange terms between nonequivalent electrons and the nondiagonal Lagrange multipliers arising from the orthogonality requirement. Afterwards we shall consider the special case of a He-like ion, the discussion being possibly extended to more complex ions without any difficulties.

The number density for the bound electrons $\rho_b(r)$ can be written in terms of the radial wave functions, solutions of Eq. (8), and of the energies $E(\nu LS)$ relative to the state with the configuration $\nu=nln'l'$, the total angular momentum L, and the total spin momentum S as

$$\rho_b(r)=\left[\sum_{\nu LS}b_\nu(LS)\rho_{\nu LS}(r)\right]\left[\sum_{\nu LS}(b)\right]^{-1} , \tag{9}$$

where

$$b_\nu(LS)=(2L+1)(2S+1) \times\exp\{-[E(\nu LS)-E(1s^2)]/kT_e\} .$$

Here we consider the central charge $Z\leq 15$ and then suppose that the relativistic effects can be treated as a perturbation in LS coupling. The radial density function $\rho_{\nu LS}(r)$ is given by

$$\rho_{\nu LS}(r)=\sum_{j=1}^{M}q_jp_j^2(r)(4\pi r^2)^{-1} , \tag{10}$$

where q_j stands for the number of electrons in the subshell j. According to Eq. (9), we note that the density $\rho_b(r)$ integrated over the ion sphere gives the total number of bound electrons N. In Eq. (9), the summation concerns the group of states the radiative lifetime of which is larger than the collisional relaxation time. To minimize computer time, we can also deal with the average atomic potential[3,7] by considering the summation over all bound states. In fact, we have verified that the discrepancy be-

tween the two above-mentioned summation methods is within 3% for the Ne IX resonance line shift.

Then, in order to obtain the atomic and plasma parameters, we have to solve self-consistently, for any given N_e and T_e, the Poisson equation (1) with the confinement condition (7) and the wave equation (8) for all bound states ($nln'l'^{2S+1}L$). The calculation of the number density $\rho_b(r)$, Eq. (9), necessitates solving the eigenvalue problem, Eq. (8), for simply and doubly excited states. In the dense region of plasmas, the latter can be, in fact, omitted because their populations are small in comparison with those of the ground state and they lie above the first ionization limit so that the statistical weight $b(\nu LS)$ becomes negligible.

Concerning the simply excited states ($\alpha = 1snl, LS$), it is convenient to express their energy in the following form:[22]

$$E(\alpha LS) = E_{\rm av}(\alpha L) + \Delta E(\alpha LS) , \tag{11}$$

where $E_{\rm av}(\alpha L)$ denotes the average energy of the given configuration αL and $\Delta E(\alpha LS)$ and its deviation which is directly related to the Slater exchange integrals G^L

$$\Delta E(\alpha LS) = (-1)^S \frac{3}{2} \frac{G^L(1s,nl)}{(2L+1)(2S+1)} . \tag{12}$$

In general, this term satisfies the following inequalities:

$$\begin{aligned} &\Delta E(\alpha LS) \ll E_{\rm av}(\alpha L) , \\ &\Delta E(\alpha LS) \ll kT_e . \end{aligned} \tag{13}$$

Therefore, the number density of the bound electrons $\rho_b(r)$, Eq. (9), can be calculated by using the average energy and corresponding wave function for each atomic configuration. The distinction between singlet and triplet states in the wave, Eq. (8), is necessary only at the final step when self-consistency is already ensured for the effective atomic potential

$$V_A(r) = -\frac{Z}{r} + \int_{r'<R_0} \frac{\rho_e(r')d\mathbf{r}}{|\mathbf{r}-\mathbf{r}'|} . \tag{14}$$

The latter has been obtained according to the same numerical procedure as described for H-like ions in Ref. 3. Here, by using the above-mentioned average configuration approximation (ACA), which allows significant reduction of the number of states of interest in Eq. (9), we note that the computer time remains acceptable in spite of a more complicated atomic structure. We can check the precision of this approximation by examining Table I where we note that the relative discrepancy between the transition energies calculated with detailed multiplet states and those obtained with average configurations does not exceed 10^{-5}.

Plasma effects on the fundamental and singly excited singlet levels of Ne IX are illustrated in Tables II and III. For a fixed temperature ($T = 500$ eV) and increasing electron density N_e, Table II shows that (i) the number of bound states decreases rapidly. In fact, no bound state with $n = 4$ and 3 exists when N_e goes beyond 10^{23} and 10^{24} cm^{-3} respectively. (ii) All the energy levels move more and more towards the continuum. Besides, the energy shift, counted from the unperturbed value, increases with increasing orbital quantum number L and decreasing principal quantum number n. The latter fact provides for a red line shift which will be discussed together with the collisional results given in Sec. III.

TABLE I. Transition energies (in Ry) of the Ne IX He_α line calculated with $T_e = 500$ eV and various N_e by using (a) detailed multiplet states and (b) average atomic configurations.

N_e \ ω	(a)	(b)
0	67.6264	67.6264
3.10^{23}	67.5222	33.5227
10^{24}	67.2895	67.2911
3.10^{24}	66.7222	66.7268

Table III gives level energy values for a fixed density $N_e = 10^{24}$ cm^{-3} and various temperatures, the last line being obtained by using the uniform electron gas model (UEGM), i.e., by replacing $\rho_e(r)$ by N_e in Eq. (14). As the temperature increases we note that energy levels become deeper and deeper and tend towards the limit values given by the UEGM.[3,8] This can be explained by pointing out that the lower the temperature, the more efficient the nuclear Coulomb attraction and, consequently, the larger the fractional number of free electrons compressed in an atomic orbit. Also, as the total number of electrons is preserved according to the electrical neutrality condition, Eq. (7), the boundary electron density $\rho_e(R_0)$ is smaller than the volume-averaged N_e. Indeed, as shown in the second line of Table II, or the second column of Table III, the ratio $\rho_e(R_0)/N_e$ decreases significantly when N_e increases or T_e decreases, respectively.

In connection with the previous plasma polarization effects, some internal atomic properties are worth commenting on. The first property is the separation between singlet and triplet energy levels,

$$E_{\rm ex}(\alpha L) = E(\alpha\,{}^1L) - E(\alpha\,{}^3L) = \frac{2G^L(\alpha)}{(2L+1)} , \tag{15}$$

which allows us to determine the position of the intercombination lines, often suggested as spectroscopic probes,[23] with regard to the resonance lines. As an example, curve (*b*) in Fig. 1 represents the density dependence of this exchange energy, relative to the unperturbed value, for the $1s2p$ level. We can clearly see that this quantity is much smaller [curve (*b*) is multiplied by a factor of 10] than the plasma polarization shift of the corresponding resonance line, shown in curve (*a*). So, instead of systematically solving Eq. (8) with the self-consistent potential V_A, Eq. (14), we can deduce the triplet energy levels from the singlet ones by replacing the right-hand side of Eq. (15) with its unperturbed values. A detailed examination of Table II shows that this assertion is true for all other cases up to $n = 4$.

Another internal atomic property is the correlation energy E_c which is neglected in the Hartree-Fock theory. Denoting by E and $E_{\rm HF}$ the "exact" and Hartree-Fock

TABLE II. Variation of the Ne IX energy levels ($-E$ in Ry) with the electron density N_e for a given temperature $T_e = 500$ eV.

N_e (cm^{-3})	0	6×10^{22}	10^{23}	3×10^{23}	6×10^{23}	10^{24}	3×10^{24}	6×10^{24}
$\rho_e(R_0)/N_e$	1	0.978	0.975	0.969	0.964	0.960	0.949	0.944
$1s^2\,{}^1S$	187.722	179.532	177.893	173.391	169.510	166.006	155.905	147.226
$1s2s\,{}^1S$	121.230	113.067	111.446	107.029	103.274	99.932	90.516	82.199
$1s2s\,{}^3S$	121.333	113.170	111.549	107.132	103.376	100.033	90.615	82.300
$1s2p\,{}^1P$	120.096	111.927	110.302	105.869	102.088	98.715	89.179	80.876
$1s2p\,{}^3P$	120.626	112.456	110.830	106.383	102.607	99.206	89.670	81.389
$1s3s\,{}^1S$	109.237	101.167	99.606	95.478	91.954			
$1s3s\,{}^3S$	109.301	101.229	99.668	95.537	92.016			
$1s3p\,{}^1P$	108.961	100.882	99.317	95.165	91.632			
$1s3p\,{}^3P$	109.107	101.025	99.457	95.296	91.768			
$1s3d\,{}^1D$	108.998	100.888	99.302	95.060	91.500			
$1s3d\,{}^3D$	109.004	100.894	99.308	95.065	91.505			
$1s4s\,{}^1S$	105.556	97.314	95.866					
$1s4s\,{}^3S$	105.187	97.341	95.893					
$1s4p\,{}^1P$	105.047	97.195	95.743					
$1s4p\,{}^3P$	105.107	97.248	95.795					
$1s4d\,{}^1D$	105.061	97.159	95.694					
$1s4d\,{}^3D$	105.065	97.162	95.697					
$1s4f\,{}^1F$	105.062	97.086	95.586					
$1s4d\,{}^3F$	105.063	97.086	95.586					

energies, respectively, the correlation energy is defined by

$$E = E_{\mathrm{HF}} + E_c \ . \tag{16}$$

In this paper, E has been obtained by using a multiconfigurational method in which the complete wave function basis is defined in terms of natural orbitals.[24,25] This method allows us to significantly reduce the number of configurations occurring in the total wave-function expansion. Numerical results for $E_c(1s^2\,{}^1S)$ and $E_c(1s2p\,{}^1P)$ are given in Table IV where we note that their density dependence is actually negligible. Therefore, to obtain the self-consistent exact energy E, we can use the Hartree-Fock energy solution of Eqs. (1), (7), (8), and (11) and replace E_c by its unperturbed value E_c^0. Finally, for $Z \geq 15$, we note that Eq. (16) can be improved by adding to the right-hand side the relativistic corrections calculated for isolated ions. This is justified by the fact that plasma polarization is a volume-averaged effect while relativistic effects are localized near the nucleus.

III. ELECTRON RELAXATION OPERATOR

The confined atom model, described in Sec. II, provides us with very useful parameters such as free-electron density, energy, and wave functions of bound states, etc., but does not allow us to obtain the linewidth which is an essential quantity in plasma spectroscopy. The perturbing electrons alter the radiator by successive collisions which interrupt more or less often the emission. As we have already pointed out, the effective atomic lifetime is generally much larger than the inverse of the electron plasma frequency ω_p^{-1} so electron interaction can be treated by the impact approximation. As the close collisions become more important as the density increases, we use in this paper a quantum-mechanical method to evaluate the electron relaxation operator defined by[26]

$$\Gamma_e = \pi N_e \left\langle \frac{1}{v} \mathcal{T} \right\rangle_{\mathrm{av}} , \tag{17}$$

where $\mathcal{T}$ denotes a generalized transition operator acting

TABLE III. Variation of the Ne IX levels ($-E$ in Ry) with the temperature T_e for a given density $N_e = 10^{24}$ cm^{-3}.

T_e (eV)	$\rho_e(R_0)/N_e$	$1s^2\,{}^1S$	$1s2s\,{}^1S$	$1s2p\,{}^1P$
100	0.898	163.350	97.533	96.274
200	0.930	164.767	98.813	97.576
400	0.954	165.763	99.713	98.492
600	0.965	166.179	100.088	98.874
800	0.971	166.414	100.298	99.088
1000	0.975	166.565	100.434	99.227
1200	0.977	166.672	100.530	99.324
1500	0.980	166.784	100.630	99.426
∞	1	167.270	101.070	99.872

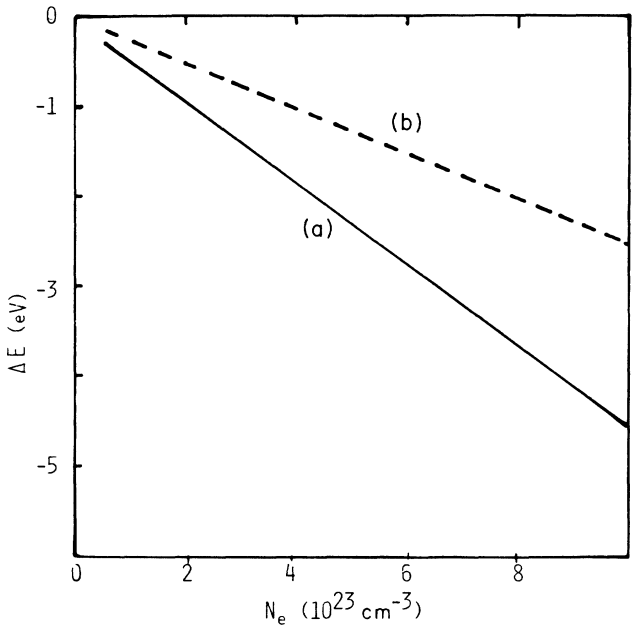

FIG. 1. Density variation of the shift calculated with a given temperature $T_e=500$ eV. ——, for the resonance He_α line of Ne IX; — — —, for the exchange energy (15) of the $1s2p$ level. Here the data have been multiplied by a factor of 10.

in Liouville space. The thermal average is performed assuming a Maxwellian distribution for the electron velocity. For the He-like principal spectral series, the relaxation operator Γ_e is diagonal and can be expressed in terms of the transition-matrix elements in the coupled representation[3]

$$\Gamma_e(\mathrm{if})=\pi N_e\left\langle\frac{1}{V}\sum_{lL_l^T}[T_{L_l^T}(\nu_i,\nu_i)+T_l^+(\nu_f,\nu_f) - T_{L_l^T}(\nu_i,\nu_i)T_l^+(\nu_f,\nu_f)]\frac{(L_l^T)}{(L_i)}\right\rangle_{\mathrm{av}} \tag{18}$$

where i,f refer to the upper $(1snl_i\,{}^1L_i)$ and lower $(1s^2\,{}^1S)$ levels of the transition, respectively, and ν indicates the set of quantum numbers $\nu=(nLklL^T)$ specifying the collision channel. L^T stands for the total angular momentum ($\mathbf{L}^T=\mathbf{L}+\boldsymbol{l}$).

TABLE IV. Correlation energy calculated with $T_e=500$ eV and various N_e. The calculation includes all the configuration states which give 80% of the unperturbed value E_c^0.

N_e	$E_c(1s^2\,{}^1S)$	$E_c(1s2p\,{}^1P)$
0	−0.036 57	−0.005 77
1×10^{23}	−0.036 57	−0.005 77
3.10^{23}	−0.036 57	−0.005 72
6.10^{23}	−0.036 57	−0.005 66
1.10^{24}	−0.036 57	−0.005 59

The real and imaginary parts of Γ_e give, respectively, the linewidth and the line shift due to collisions between free electrons and the target radiator

$$\Gamma_e=W_e-iD_e\ . \tag{19}$$

Owing to the optical theorem, W_e can be expressed in terms of cross sections connecting the level of interest (i or f) with all the states of discrete and continuous spectra. On the other hand, a direct calculation of the elastic T matrix elements is the only way to obtain the shift D_e. In order to calculate those scattering data, we have already noted[3,26] that the electron temperature and radiator charge number in laser plasmas are high enough to ensure the validity of the Coulomb-Born-Oppenheimer (CBO) approximation. The latter will be used here in its unitarized version[3,27] by writing the transition matrix in the form $T=-2iR/(1-iR)$, where R is the real and symmetrical reactance matrix whose elements have been specified for He-like ions in Ref. 28.

The calculation of various matrix elements has been performed by using the following.

(1) For the ground state in which the two electrons have the same orbital and opposite spins, the suitably parametrized wave function given by Clementi and Roetti[29] on the basis of a Hartree-Fock calculation.

(2) For excited states, Coulomb wave functions defined in the framework of quantum-defect theory. This approximation allows us to save significant computer time without losing precision if the number of charges is relatively high. This is clearly seen in Table V where some collision strengths of O VII are given in the basis or either quantum-defect or Hartree-Fock theory.[30]

The evaluation of the linewidth has been performed in such a way to include properly strong collisions which play a leading part in high-density plasmas. As the He-like atomic levels are not degenerate with respect to the orbital momentum L, the dipolar cross sections do not present a logarithmic divergence at large impact parameters. Therefore, in a first step we can ignore electron correlation effects and define a total width W_e^T which has been obtained as follows.

We calculate all the transitions $(n\,{}^1L\rightarrow n'\,{}^1L)$ with $n,n'\leq5$ by using the CBO approximation and including interactions between the free and bound electrons up to the octopole term. The summation in the partial-wave expansion is performed up to the perturber orbital quantum number l_0 which is high enough to ensure the validity of the dipolar interaction for $l\geq l_0$. The other bound-bound and bound-free cross sections are deduced from an approximate formula[31] where the ionization potential lowering and the internal electron screening are properly included.

When the perturber angular momentum is high enough, only the long-range part of the direct potential Y_λ is important because the centrifugal barrier prevents interaction with the short-range part. So we can write

$$Y_\lambda(a,a';r)\simeq S_\lambda(a,a')r^{-(\lambda+1)}\ , \tag{20}$$

where $S_\lambda(a,a')$ represents a multipolar radial integral

TABLE V. Collision strengths relative to O VII $2\,^1S \rightarrow n\,^1P$ transitions obtained by means of the Coulomb-Born approximation with various target wave functions. (a) Quantum-defect theory (our results) and (b) Hartree-Fock method (Ref. 30). Impact energies (X) are in threshold units.

	$n=2$		$n=3$		$n=4$	
X	(a)	(b)	(a)	(b)	(a)	(b)
1	2.72	2.78	0.062	0.062	0.0154	0.0154
2	2.85	2.90	0.120	0.122	0.0302	0.0303
4	3.08	3.13	0.209	0.204	0.0493	0.0496

$$S_\lambda(a,a')=\int_0^\infty P_a(r)P_{a'}(r)r^\lambda dr \ .$$

In fact, as already mentioned, for $l \geq l_0$ only the dipolar term with $\lambda=1$ is needed and we can use the Coulomb-Bethe approximation for its calculation. Under these conditions it is more interesting to develop the inelastic collision strengths $\Omega_{\rm in}=\sigma_{\rm in}E/\pi$ in terms of a complete summation over partial waves

$$\Omega_{\rm in}(\nu_a L \rightarrow \nu'_a L')=\sum_{L^T}\Omega_{L^T}(\nu_a L \rightarrow \nu'_a L') \ ,$$

$$=\sum_{L^T=0}^{L_0^T}[\Omega_{L^T}(\nu_a L \rightarrow \nu'_a L')-\Omega_{L^T}^{\text{C-Be}}(\nu_a L \rightarrow \nu'_a L')]+\Omega_T^{\text{C-Be}}(\nu_a L \rightarrow \nu'_a L') \ . \tag{21}$$

Here L_0^T is the total angular momentum corresponding to the perturber momentum $l_0=40$ and C-Be denotes Coulomb-Bethe. The first term on the right-hand side of Eq. (21) is directly obtained in our CBO code. The second one can be written in the following form:[32]

$$\Omega_T^{\text{C-Be}}(\nu_a L \rightarrow \nu'_a L')=\tfrac{16}{3}l_{a>}S_1^2(a,a')B_0 \ , \tag{22}$$

where B_l is a Gaunt factor given by

$$B_l=\{[1+(l+1)^2K^2]I_1^2(K,l+1;K',l)-[1+(l+1)K'^2]I_1(K,l;K'l+1)]\}[(l+1)(K^2-K'^2)]^{-1} \ . \tag{23}$$

Here K (or K') stands for $(Z-2)^{-1}k$ (or k'). I_1 is the Coulomb integral which involves[27] confluent hypergeometric functions ${}_1F_1$. It is easy to show that only the two terms $I_1(K,0;K',1)$ and $I_1(K,1;K',0)$ are needed, the others being deduced by means of simple recurrence relations.

Then by using the scaling law relative to radiator charge number, the total linewidth for He-like principal series lines can be written as

$$W_e^T(nl_i\,{}^1L)=\frac{\pi}{2}\frac{N_e}{(l_i)}\left\langle\frac{1}{v}\left[\sum_{\substack{\nu'_a \\ a=i,f}}\Omega_{\rm in}(\nu_a L \rightarrow \nu'_a L')+\Omega^{\rm el}(i,f;L)\right]\right\rangle_{\rm av}$$

$$=\pi^{1/2}\tilde{N}_e\tilde{T}_e^{-1/2}Q^T(nl_i,T_e) \tag{24}$$

in a.u., where

$$\tilde{N}_e=N_e(\text{a.u.})/Z_{\rm eff}^3;\tilde{T}_e=T_e(\text{Ry})/Z_{\rm eff}^2$$

and $Z_{\rm eff}=Z-\sigma_{nl_i}$ is the effective charge acting on the outer atomic electron (nl_i). $\Omega_{\rm el}$ denotes the elastic collision strengths for upper (i) and lower (f) levels including the interference term.[33]

For highly charged ions ($Z \geq 10$), the screening parameter σ_{nl_i} can be approximated by unity. In Eq. (24), Q^T is a coefficient obtained by averaging over the reduced incident energy $u=mv^2/2kT_e$

$$Q^T(nl_i,T_e)=\int_0^\infty e^{-u}\left[\frac{Z_{\rm eff}^2}{(l_i)}\left[\sum_{\substack{\nu'_a \\ a=i,f}}\Omega_{\rm in}(\nu_a L \rightarrow \nu'_a L')+\Omega_{\rm el}(i,f;L)\right]\right]du \ . \tag{25}$$

Calculation shows that this coefficient is nearly independent of Z. Q^T is given in Table VI as a function of temperature and atomic quantum numbers.

To obtain the effective linewidth, we have to exclude from $W_e^T(nl_i\,{}^1L)$, Eq. (24), the contribution of large relative orbital quantum numbers $l > l_{\max}$ where the cutoff value $l_{\max}$ is given by[13]

$$l_{\max}(l_{\max}+1)=4E^2/m\hbar^2(\omega_p^2+\Delta\omega^2+\Delta\omega_S^2)\ . \tag{26}$$

Here, the presence of the plasma frequency $\omega_p=(4\pi eN_e/m)^{1/2}$, the frequency separation from the unperturbed line $\Delta\omega$, and the frequency shift due to quasistatic perturbations $\Delta\omega_S$ allow for screening of electron fields and the finite duration of collisions and level splittings, respectively. Then, the effective linewidth can be written as

$$W_e(nl_i\,{}^1L)=\pi^{1/2}\tilde{N}_e\tilde{T}_e^{-1/2}\times[Q^T(nl_i,T_e)-Q^S(nl_i,T_e,N_e)]\ , \tag{27}$$

in a.u. where the screened part $Q^S(nl_i,T_e,N_e)$ is defined by Eq. (27) with the term in square brackets replaced by the following partial Coulomb-Bethe collision strength:

$$\Omega_{l_{\max}}^{\text{C-Be}}(\nu_aL)=\sum_{L^T=l_{\max}}^{\infty}\sum_{\nu_a'}\Omega_{L^T}^{\text{C-Be}}(\nu_aL\rightarrow\nu_a'L')$$
$$\equiv\tfrac{16}{3}\sum_{a'}l_{a>}S_1^2(a,a')B_{l_{\max}}\ . \tag{28}$$

Here, the Gaunt factor $B_{l_{\max}}$ is given in a closed form, Eq. (23), where the electron density and the correction to impact approximation occur only via the cutoff orbital quantum number $l_{\max}$, Eq. (26).

A comparison between the total part Q^T and screened part Q^S of the linewidth is given in Table VII with the assumption $|\Delta\omega|,\ |\Delta\omega_S|<\omega_p$. As expected, we can see that Q^S increases when the Debye radius $\rho_D=(4\pi N_e e^2/kT)^{1/2}$ decreases. Furthermore, we note that the ratio Q^S/Q^T increases rapidly with the principal quantum number of atomic states. This behavior of cross sections for highly excited states is not surprising because they imply a notable contribution of partial waves with large orbital quantum numbers and are consequently very sensitive to the cutoff procedure defined by Eq. (26).

If we consider the scaling law relative to the radiator charge number, the electron line shift D_e, given by Eqs. (18) and (19), can be written as

$$D_e(nl_i\,{}^1L)=2\pi^{1/2}\tilde{N}_e\tilde{T}_e^{-1/2}Z_{\text{eff}}\Delta(nl_i,T_e)\ , \tag{29}$$

where, similarly to the linewidth coefficient Q^T, the line-shift coefficient Δ is a sensitive function of electronic temperature and of atomic quantum numbers. As shown in Table VIII, giving $\Delta(nl_i,T_e)$ with $Z_e=10$, we note the following. $\Delta(nl_i,T_e)$ increases with electron temperature and tends towards a finite value $\Delta(nl_i,\infty)$ which corresponds to the uniform electron-gas model [see Eq. (9) of Ref. 3]. As an example, Fig. 2 shows the Ne IX He_α line shift calculated with $N_e=10^{24}$ cm^{-3} and various temperatures.

TABLE VI. Temperature dependence of the collision coefficient $Q^T(nl,T_e)$ defining the total linewidth $W_e^T(nl\,{}^1L)$ [Eq. (24)].

$\tilde{T}_e$ (Ry)	$Q^T(2S)$ $\times10^{-2}$	$Q^T(2P)$ $\times10^{-2}$	$Q^T(3S)$ $\times10^{-3}$	$Q^T(3P)$ $\times10^{-3}$	$Q^T(3D)$ $\times10^{-3}$	$Q^T(4S)$ $\times10^{-3}$	$Q^T(4P)$ $\times10^{-3}$	$Q^T(4D)$ $\times10^{-3}$	$Q^T(4F)$ $\times10^{-3}$
0.02	1.857	0.790	1.292	1.147	0.512	4.524	4.801	4.848	2.348
0.04	1.983	0.830	1.421	1.289	0.594	5.092	5.446	5.507	2.647
0.06	2.087	0.872	1.517	1.386	0.650	5.470	5.840	5.848	2.796
0.08	2.178	0.916	1.592	1.461	0.692	5.764	6.150	6.134	2.920
0.10	2.259	0.961	1.649	1.518	0.724	5.979	6.369	6.331	3.003
0.12	2.336	1.006	1.704	1.574	0.760	6.169	6.562	6.499	3.078
0.14	2.406	1.047	1.751	1.619	0.785	6.335	6.733	6.649	3.141
0.16	2.470	1.088	1.791	1.656	0.806	6.474	6.876	6.771	3.190
0.18	2.529	1.127	1.825	1.686	0.822	6.591	6.992	6.868	3.228
0.20	2.583	1.164	1.854	1.711	0.835	6.688	7.087	6.942	3.255
0.25	2.697	1.232	1.916	1.762	0.858	6.889	7.279	7.079	3.299
0.30	2.799	1.297	1.974	1.814	0.886	7.082	7.470	7.225	3.353
0.35	2.887	1.357	2.022	1.857	0.910	7.250	7.630	7.349	3.401
0.40	2.966	1.413	2.061	1.894	0.931	7.385	7.758	7.448	3.438
0.45	3.043	1.473	2.098	1.927	0.951	7.488	7.858	7.524	3.468
0.50	3.113	1.528	2.132	1.957	0.969	7.564	7.934	7.584	3.491
0.55	3.173	1.569	2.164	1.985	0.987	7.666	8.028	7.653	3.518
0.60	3.228	1.606	2.192	2.011	1.003	7.768	8.115	7.714	3.541
0.65	3.278	1.639	2.217	2.034	1.017	7.860	8.191	7.766	3.562
0.70	3.324	1.668	2.238	2.054	1.023	7.945	8.264	7.817	3.581
0.75	3.367	1.695	2.257	2.073	1.039	8.022	8.033	7.864	3.598
0.80	3.405	1.718	2.274	2.089	1.049	8.090	8.388	7.905	3.614
0.85	3.440	1.740	2.290	2.104	1.057	8.143	8.438	7.943	3.627
0.90	3.473	1.760	2.304	2.117	1.064	8.186	8.481	7.977	3.639
0.95	3.503	1.778	2.318	2.129	1.071	8.222	8.519	8.006	3.650
1.00	3.530	1.795	2.330	2.140	1.077	8.250	8.551	8.032	3.659

TABLE VII. Relative contribution to the electron linewidth $W_e(nl\,^1L)$ [Eq. (27)] of Q^1 (first line) and of Q^S (second line). The data are given for the Ne IX in units of Z_{eff}^2.

$nl\,^1L$	$N_e=1.10^{22}$ cm^{-3} $T_e=385$ eV $\rho_{\max}=27.58$	$N_e=1.10^{22}$ cm^{-3} $T_e=220$ eV $\rho_{\max}=20.87$	$N_e=5.10^{22}$ cm^{-3} $T_e=661$ eV $\rho_{\max}=16.16$	$N_e=5.10^{22}$ cm^{-3} $T_e=385$ eV $\rho_{\max}=12.34$
$2s\,^1S$	3.56	3.19	3.98	3.56
	0.13	0.14	0.49	0.52
$2p\,^1P$	1.67	1.44	1.98	1.67
	0.04	0.05	0.17	0.18
$3s\,^1S$	24.96	22.89	27.06	24.96
	4.84	5.07	8.91	9.13
$3p\,^1P$	22.93	21.13	24.83	22.93
	6.69	6.88	9.83	9.96
$3d\,^1D$	11.24	10.31	12.38	11.24
	3.03	3.09	4.11	4.13
$4s\,^1S$	89.51	82.57	95.90	89.51
	30.98	31.90	45.42	45.94
$4p\,^1P$	94.21	87.50	100.18	94.21
	37.85	38.09	50.20	50.50
$4d\,^1D$	90.74	85.71	95.24	90.74
	37.85	38.09	46.37	46.42
$4f\,^1F$	41.99	40.19	43.72	41.99
	15.27	15.31	18.11	18.12

TABLE VIII. Variation of the electron shift coefficient $\Delta(nl, T_e)$ with temperature.

$\tilde{T}_e$ (Ry)	$\Delta(2S)$	$\Delta(2P)$	$\Delta(3S)$	$\Delta(3P)$	$\Delta(3D)$	$\Delta(4S)$	$\Delta(4P)$	$\Delta(4D)$	$\Delta(4F)$
0.02	18.4	14.9	65.8	60.9	47.8	155.2	148.6	130.7	106.2
0.04	18.8	15.2	69.0	63.7	49.5	168.2	161.2	141.1	112.5
0.06	19.2	15.4	71.8	66.2	51.0	179.1	171.6	149.5	117.8
0.08	19.5	15.6	74.4	68.5	52.4	188.9	181.0	157.2	122.7
0.10	19.9	15.9	76.7	70.6	53.7	197.8	189.4	164.1	127.2
0.12	20.2	16.1	79.0	72.5	55.0	206.0	197.2	170.5	131.5
0.14	20.5	16.3	81.1	74.5	56.2	214.0	204.7	176.7	135.6
0.16	20.8	16.5	83.2	76.3	57.3	221.5	211.8	182.5	139.4
0.18	21.1	16.7	85.1	78.0	58.5	228.5	218.5	188.0	143.1
0.20	21.4	16.9	87.0	79.7	59.5	235.3	224.9	193.3	146.7
0.25	22.1	17.4	91.5	83.6	62.1	251.1	239.8	205.5	155.1
0.30	22.8	17.9	95.7	87.4	64.5	265.9	253.8	217.1	162.9
0.35	23.4	18.3	99.6	90.9	66.8	279.5	266.9	227.8	170.3
0.40	24.0	18.7	103.3	94.2	69.0	292.0	278.9	237.7	177.1
0.45	24.5	19.1	106.8	97.3	71.0	303.5	290.1	246.9	183.5
0.50	25.1	19.6	110.2	100.3	73.0	314.4	300.7	255.6	189.6
0.55	25.7	20.0	113.5	103.3	75.0	324.9	311.0	264.2	195.6
0.60	26.2	20.3	116.5	106.0	76.8	334.6	320.7	272.2	201.2
0.65	26.8	20.7	119.5	108.8	78.5	343.7	330.0	279.8	206.6
0.70	27.3	21.1	122.4	111.4	80.3	352.5	339.0	287.3	211.9
0.75	27.8	21.4	125.3	114.0	82.0	361.0	347.7	294.6	217.1
0.80	28.2	21.8	128.1	116.5	83.7	369.0	356.0	301.6	222.1
0.85	28.7	22.1	130.8	119.0	85.3	376.8	364.1	308.3	227.0
0.90	29.2	22.4	133.4	121.4	86.9	384.3	371.9	314.9	231.8
0.95	29.6	22.7	136.1	123.8	88.5	391.4	379.4	321.3	236.5
1.00	30.1	23.1	138.6	126.2	90.1	398.2	386.7	327.5	241.1

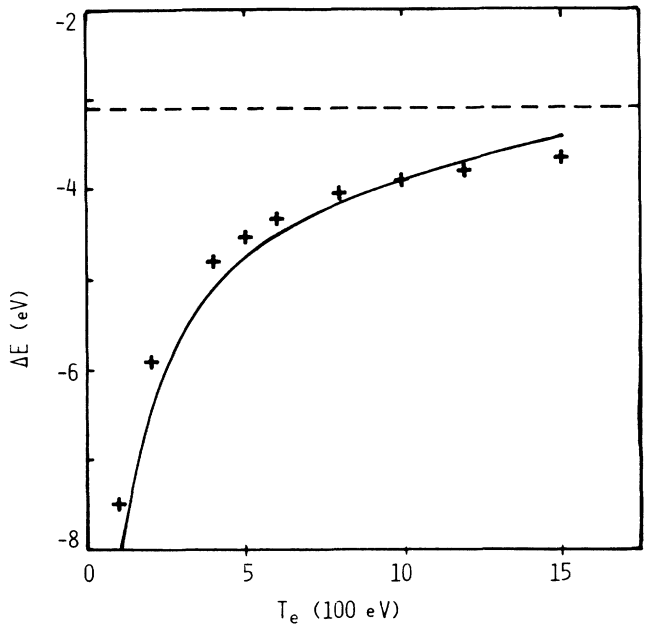

FIG. 2. Temperature dependence of the Ne IX He_α line shift calculated with $N_e=10^{24}$ cm^{-3}. $\times\times\times$, confined atom model; ——, impact theory with the reduced density, $\rho_e(R_0)$, Eq. (6); — — —, uniform electron gas model.

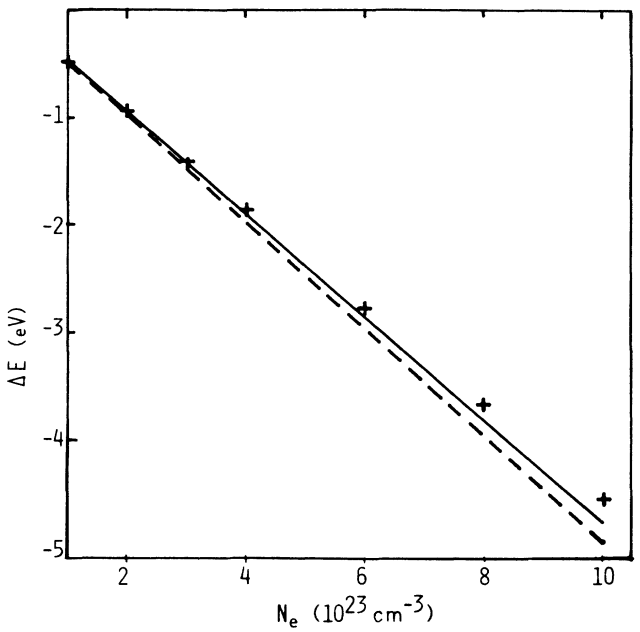

FIG. 3. Density dependence of the Ne IX He_α line shift calculated with $T_e=500$ eV. $\times\times\times$, confined atom model; ——, impact theory with the reduced density, $\rho_e(R_0)$, Eq. (6); — — —, impact theory with the mean density N_e.

$\Delta(nl_i, T_e)$ decreases smoothly with the increasing orbital quantum number l_i and varies approximately as the fourth power of the principal quantum number n. This behavior is consistent with the r^2 dependence of the monopolar interaction which prevails at high temperature. Indeed, numerical calculation has shown that dipolar and other long-range interactions have negligible contributions to the line shift. As a consequence, we note that, in contrast with Eq. (27), Eq. (29) has no shielded term. However, due to the fact that collisions start at the boundary atomic surface, it is advisable to replace in Eq. (29) the volume averaged density N_e by the depressed one, $\rho_e(R_0)$ [see Eq. (6)]. This is indeed equivalent to a coupling effect between the radiator and thermal bath already suggested by Royer.[34] Figure 3 shows that the line shift given by the quantum-mechanical impact theory including the boundary depression effect is in very good agreement with the corresponding transition energy deduced from the confined atom model.

Comparing Table II, Fig. 2, and Fig. 3 to Table I, Fig. 6, and Fig. 4 of Ref. 3, respectively, we point out that the ratio of the line shift in He-like ions to that in H-like ions is $[Z/(Z-\eta)]^2$ where η is close to unity and expresses essentially the shielding effect of the internal bound electron in He-like ions. On the other hand, we note that our results are 20% larger than those given by Skupsky and Davis and Blaha[7] who considered free electrons and ions together in their self-consistent-field calculation. In fact, as we have mentioned at the beginning of Sec. II, the ion component is characterized by a very long relaxation time and should be treated separately in line-broadening problems.

To compare our results to those based on density-functional theory,[35,36] we consider a plasma with $N_e=10^{24}$ cm^{-3}, $T_e=400$ eV, and enclosing H-like and He-like ions in the respective proportions 0.77 and 0.23 (so that the average number of bound electrons is $Z-\bar{Z}=1.23$). In the framework of our model, we have obtained the transition energy $\omega_H=74.697$ Ry and $\omega_{He}=67.271$ Ry for the Ne X H_α and Ne IX He_α lines, respectively. The average transition energy of the resonance line is then $\bar{\omega}=0.77\omega_H+0.23\omega_{He}=72.989$ Ry. We note that this value lies between the values 72.74 and 73.73 Ry given by Cauble, Blaha, and Davis[36] using the Boltzmann hypernetted-chain approximations, respectively.

IV. CONCLUSION

In this paper we developed a confined atom model for describing the atomic structure of many-electron ions immersed in dense plasmas. We have shown that self-consistent parameters, such as the total electrostatic potential and electronic energy levels, can be obtained with precision by means of an average configuration approximation. Furthermore, in connection with plasma effects, we have investigated correlation and exchange energies which are characteristic of many-electron atoms. For the temperature and density range of plasma regions where x-ray radiation is intense, we have used a multiconfigurational calculation and found that the correlation energy is indeed independent of the local plasma conditions (Table IV). The same statement is true for the exchange energy (Fig. 1). This behavior can be ex-

plained by noting that the nuclear attraction potential $-Z/r$ is effectively screened by surrounding free particles of plasmas only at large distance while the two above-mentioned atomic parameters are mostly linked to small r values.

In Sec. III we have considered the perturbation of atomic states due to electron collisions. The so-called electron relaxation operator Γ_e, Eq. (17), is treated by including quantum mechanically all multipolar orders of Coulomb interaction. As shown in Eq. (27), the linewidth $W_e = \mathrm{Re}\Gamma_e$ has been expressed as the difference between the total part Q^T, where, in particular, cross sections relative to penetrating orbits are properly included, and the screened part Q^S which takes into account the electron-electron correlation. The calculation of line shift $D_e = \mathrm{Im}\Gamma_e$ has been performed by directly considering the T-matrix elements. We have shown that this line shift agrees accurately with the corresponding transition energy of the above-mentioned confined atom model, provided that the boundary depression effect due to the coupling between radiator and thermal bath is taken into account. This is a typical problem where the collisional approach and the atomic model are compatible.

Concerning the relaxation operator, we made the usual approximations such as first order in electron density expansion and binary collisions to get a computable expression. But all the processes of the two-body interactions, such as, e.g., the exchange, are correctly described. On the other hand, the confined atom model can lead to high-density effects because the action and reaction between the radiator and the environment are considered. In the particular case of the He-like principal series lines, the agreement between the two theories is quite prominent with the variation of either the density or the temperature. Of course, for a suitable comparison with experiments, the complex electron collision operator given in this paper should be introduced in a complete calculation of line profiles where ion effects such as singlet-triplet mixing,[37] asymmetric broadening,[38,39] and dynamic level mixing[40] are to be taken into account.

ACKNOWLEDGMENTS

We are very grateful to R. M. More for helpful discussions during this work. Département de Recherches Physiques is "Unité Associée au Centre National de la Recherche Scientifique No. 71."

[1] M. Baus and J. P. Hansen, Phys. Rep. **59**, 1 (1980).
[2] R. M. More, in *Atomic and Molecular Physics of Controlled Thermonuclear Fusion,* edited by C. Joachain and D. Post (Plenum, New York, 1983), p. 399.
[3] H. Nguyen, M. Koenig, D. Benredjem, M. Caby, and G. Coulaud, Phys. Rev. A **33**, 1279 (1986).
[4] H. R. Griem, *Spectral Line Broadening by Plasmas* (Academic, New York, 1974).
[5] P. Lemaire, P. Jaeglé, and A. Carillon, Ann. Phys. (Paris) Colloq. **11**, C3-61 (1986).
[6] K. G. H. Baldwin, J. R. Liu, J. D. Kilkenny, and D. D. Burgess, J. Phys. B **19**, L179 (1986).
[7] S. Skupsky, Phys. Rev. A **21**, 1316 (1980); J. Davis and M. Blaha, J. Quant. Spectrosc. Radiat. Transfer **27**, 307 (1982).
[8] D. Salzmann and H. Szichman, Phys. Rev. A **35**, 805 (1987).
[9] J. D. Kilkenny, R. W. Lee, M. H. Key, and J. G. Lunney, Phys. Rev. A **22**, 2746 (1980).
[10] B. Yaakobi, S. Skupsky, R. L. McCrony, C. F. Hooper, H. Deckman, P. Bourke, and J. M. Soures, Phys. Rev. Lett. **44**, 1072 (1980).
[11] B. d'Etat, J. Grumberg, E. Leboucher, H. Nguyen, and A. Poquérusse, J. Phys. B **20**, 1733 (1984).
[12] R. W. Lee, B. L. Whitten, and R. E. Stout, J. Quant. Spectrosc. Radiat. Transfer **32**, 91 (1984).
[13] H. R. Griem, M. Blaha, and P. C. Kepple, Phys. Rev. A **19**, 2421 (1979).
[14] H. Nguyen, B. d'Etat, J. Grumberg, M. Caby, E. Leboucher, and G. Coulaud, Phys. Rev. A **25**, 891 (1982).
[15] R. W. Lee, G. E. Bromage, and A. E. Richards, J. Phys. B **12**, 3445 (1979).
[16] M. Baranger, Phys. Rev. **112**, 855 (1958).
[17] R. Stamm, B. Talin, E. L. Pollock, and C. A. Iglesias, *Spectral Line Shapes* (A. Deepak, Hampton, VA, 1987), Vol. 4, p. 141.
[18] D. A. Liberman, Phys. Rev. A **20**, 4981 (1979).
[19] M. W. C. Dharma-Wardana and R. Taylor, J. Phys. C **14**, 629 (1981).
[20] F. Perrot, Phys. Rev. A **20**, 586 (1979).
[21] R. M. More, Phys. Rev. A **19**, 1234 (1979).
[22] G. M. Shortley, Phys. Rev. **50**, 1072 (1936).
[23] A. H. Gabriel and C. Jordan, Case Stud. At. Collisions Phys. **2**, 209 (1972).
[24] C. Froese-Fischer, *The Hartree-Fock Method for Atoms* (Wiley, New York, 1977).
[25] P. O. Löwdin, Phys. Rev. **97**, 1479 (1955).
[26] J. M. Bañon, M. Koenig, and H. Nguyen, J. Phys. B **18**, 4195 (1985).
[27] A. Burgess, D. G. Hummer, and J. A. Tully, Philos. Trans. R. Soc. London **266**, 225 (1970).
[28] J. Davis, P. C. Kepple, and J. Blaha, J. Quant. Spectrosc. Radiat. Transfer **16**, 1043 (1976).
[29] E. Clementi and C. Roetti, At. Data Nucl. Data Tables **14**, 177 (1974).
[30] J. A. Tully and J. M. P. Serrao, Astron. Astrophys. **33**, 184 (1974).
[31] L. B. Golden and D. H. Sampson, J. Phys. B **13**, 2645 (1980).
[32] A. Burgess and W. B. Sheorey, J. Phys. B **7**, 2403 (1974); A. Burgess, *ibid.* **7**, L364 (1974).
[33] J. Banon, M. Koenig, and H. Nguyen, Phys. Lett. **101A**, 134 (1984).
[34] A. Royer, Phys. Rev. A **6**, 1741 (1972).
[35] M. W. C. Dharma-Wardana and F. Perrot, Phys. Rev. A **26**, 2096 (1982).
[36] R. Cauble, M. Blaha, and J. Davis, Phys. Rev. A **29**, 3280 (1984).
[37] H. R. Griem and P. C. Kepple, in *Spectral Line Shapes,* edited by B. Wende (de Gruyter, Berlin, 1981), Vol. 1, p. 391.
[38] B. d'Etat and H. Nguyen, in *Spectral Line Shapes,* edited by F. Rostas (de Gruyter, Berlin, 1985), Vol. 3, p. 209.
[39] R. F. Loyce, L. A. Woltz, and C. F. Hooper, Jr., Phys. Rev. A **35**, 2228 (1987).
[40] A. Calisti, R. Stamm, and B. Talin, Europhys. Lett. **4**, 1003 (1987).